Chemistry & Biology
Article

hCB2 Ligand-Interaction Landscape: Cysteine Residues Critical to Biarylpyrazole Antagonist Binding Motif and Receptor Modulation

Richard W. Mercier,[1,2,3] Ying Pei,[1,3] Lakshmipathi Pandarinathan,[2] David R. Janero,[2] Jing Zhang,[1] and Alexandros Makriyannis[2,*]
[1]School of Pharmacy, University of Connecticut, Storrs, CT 06269, USA
[2]Center for Drug Discovery, Northeastern University, Boston, MA 02115, USA
[3]These authors contributed equally to this work
*Correspondence: a.makriyannis@neu.edu
DOI 10.1016/j.chembiol.2010.08.010

SUMMARY

The human cannabinoid 2 GPCR (hCB2) is a prime therapeutic target. To define potential cysteine-related binding motifs critical to hCB2-ligand interaction, a library of hCB2 cysteine-substitution mutants and a novel, high-affinity biarylpyrazole hCB2 antagonist/inverse agonist (AM1336) functionalized to serve as a covalent affinity probe to target cysteine residues within (or in the microenvironment of) its hCB2 binding pocket were generated. The data provide direct experimental demonstration that both hCB2 TMH7 cysteines [i.e., C7.38(284) and C7.42(288)] are critical to optimal hCB2-AM1336 binding interaction and AM1336 pharmacological activity in a cell-based functional assay (cAMP formation). Elongating the AM1336 aliphatic side chain generated another novel hCB2 inverse agonist that binds covalently and selectively to C7.42(288) only. Identification of specific cysteine residues critical to hCB2 ligand interaction and function informs the structure-based design of hCB2-targeted medicines.

INTRODUCTION

As a cellular communication network ubiquitous in mammals, the endogenous cannabinoid (endocannabinoid) system influences diverse physiological processes (Di Marzo, 2009). Naturally produced cannabinergic lipids act as signaling molecules by engaging and activating at least one of two primary cannabinoid G protein-coupled receptors (GPCRs), designated CB1 and CB2. Both display the general architecture of traditional class-A GPCRs: an extracellular amino terminus; a membrane-spanning region with seven amphipathic transmembrane helices (TMHs) connected by intra- (IL) and extracellular loops (EL); and a cytoplasmic carboxyl terminus. Yet several properties distinguish CB1 and CB2, including their limited amino acid identity (44% overall and 68% within their transmembrane domains), divergent downstream effector pathways, and distinctive tissue distributions (Dalton et al., 2009; Di Marzo, 2009).

Selective modulation of CB2 signaling has the potential to address several important medical problems (Poso and Huffman, 2008). Considerable drug-discovery attention has been given to CB2 agonists, a reflection of the analgesic effect of CB2 stimulation and the recent advancement of select CB2 agonists into clinical trials for inflammatory pain (Anand et al., 2009; Rahn et al., 2008). Although CB2 blockade may promote certain pathologies (Miller and Stella, 2008), the high level of constitutive CB2 expression in immune cells, the inducibility of CB2 expression by injury stimuli even in organs (e.g., brain) with low constitutive CB2 levels, and the salutary effects of attenuating CB2 signaling in autoimmune-disease and allergy models suggest that CB2 antagonists could be important anti-inflammatory and immunomodulatory drugs (Lunn et al., 2008). Such findings suggesting the therapeutic potential of pharmacological CB2 blockade have placed increasing effort toward the discovery of highly-selective antagonists for the human CB2 GPCR (hCB2).

The integral-membrane, heptahelical nature of traditional "druggable" GPCRs including hCB2 constitutes a formidable barrier to their direct structural analysis in intact, functionally active form by classical crystallographic and spectroscopic methods (Hanson and Stevens, 2009). High-resolution structures of the vast majority of GPCRs, including CB2 from any species, are unsolved (Topiol and Sabio, 2009). Consequently, experimental definition of the hCB2 ligand-binding pocket and the mechanistic relationship between hCB2 conformational transitioning induced by ligand engagement and the receptor's functional state is lacking. Computational (mainly rhodopsin-based) homology models have served as surrogates for inferring small-molecule pharmacophoric groups and candidate hCB2 interaction domains (Durdagi et al., 2009; Tao et al., 1999). The utility of such models to the design of hCB2-targeted drugs is inherently limited by the low overall homology among class-A GPCRs and the different biochemical and molecular characteristics of rhodopsin versus hCB2 (Topiol and Sabio, 2009; Zhang et al., 2005). Further complicating definition of hCB2 ligand-binding determinants are the considerable interspecies variations in CB2 primary structure and ligand pharmacology (Liu et al., 2009; Mukherjee et al., 2004) and the ability of this GPCR to recognize cannabinergic ligands from a variety of distinct chemical classes, including prototypic tricyclic "classical" cannabinoids [e.g., the phytocannabinoid

(−)-Δ^9-tetrahydrocannabinol] (Δ^9-THC); the endocannabinoids anandamide (AEA) and 2-arachidonoylglycerol (2-AG); nonclassical cannabinoids (e.g., CP55940); aminoalkylindols (e.g., WIN55212-2); and biarylpyrazoles (e.g., SR144528) (Janero et al., 2009; Palmer et al., 2002). Experimental characterization of hCB2 binding sites for privileged structures should facilitate and inform the design and optimization of therapeutically attractive hCB2 antagonists, help refine existing CB2 computational models, and allow prediction of potential off-target activities.

The biarylpyrazole scaffold is particularly germane to the clinical translation of cannabinoid-receptor antagonists as pharmacotherapeutics. The first marketed drug to emerge from rational discovery efforts aimed at therapeutic endocannabinoid-system modulation is the biarylpyrazole CB1 blocker, rimonabant (SR141716A) (Janero and Makriyannis, 2009). A rimonabant analog, the biarylpyrazole SR144528, was the first potent, selective CB2 antagonist reported (hCB2 K_i = 0.6 nM) (Rinaldi-Carmona et al., 1998) and has served as an important pharmacological reagent for probing CB2 function (Janero et al., 2009; Lunn et al., 2008). Like SR144528, virtually all CB2-selective antagonists that have been pharmacologically characterized not only block the effects of exogenous and endogenous agonists, but also inhibit, at least in cultured cells, constitutive CB2 activity by virtue of an inverse-agonist action (Lunn et al., 2008). At (sub)molecular resolution, however, many questions surround the determinants of hCB2-ligand interaction. In this regard, the role of cysteine residues is particularly intriguing (Congreve and Marshall, 2010). Mutational and pharmacological investigations have implicated select cysteine residues in CB1 protein-protein interactions and post-translational modification and in CB2 ligand-binding competency and surface expression (Dainese et al., 2008; Gouldson et al., 2000; Kokkola et al., 2005; Shire et al., 1999; Zhang et al., 2005). These indirect experimental approaches, however, cannot demonstrate discrete hCB2-ligand interactions at the amino acid level.

To gain such insight into potential cysteine-related hCB2 ligand-binding motifs, we report application of our multidisciplinary experimental approach termed ligand assisted protein structure (LAPS), which integrates in a complementary fashion site-directed mutagenesis and the use of chemically-reactive, high-affinity covalent cannabinoid probes. Prior studies from this laboratory have established LAPS as a powerful tool for identifying critical amino acids within enzyme active sites and orthosteric GPCR ligand-binding regions (Pei et al., 2008; Picone et al., 2005; Zvonok et al., 2008; Zvonok et al., 2010). In the present investigation, we have functionalized the aliphatic side chain of a novel biarylpyrazole SR144528 analog and hCB2 inverse agonist (AM6731) with an electrophilic isothiocyanate (NCS) moiety to generate AM1336, the first covalent hCB2 antagonist/inverse agonist strategically targeted to react irreversibly with cysteine residues at (or near) its interaction site (Figure 1A). Systematic application of AM1336 as a mechanism-based covalent affinity probe to a library of single- and multiple-site hCB2 cysteine-substitution mutants (Figure 1B), along with a cell-based hCB2 functional assay, allowed us to interrogate the structural features of hCB2-antagonist interaction and, specifically, identify cysteine residues involved in hCB2 inverse-agonist engagement and function. Our results identify two hCB2 TMH7 cysteines, C7.38(284) and C7.42(288), critical to optimal AM1336 antagonist/inverse agonist binding and pharmacological activity and two others, TMH1 cysteine C1.39(40) and IL2 cysteine C137, that influence hCB2 ligand affinity or AM1336 maximum efficacy, respectively. These data augment the paucity of available experimental information on hCB2/GPCR ligand-binding regions and inform thereby the rational synthesis of hCB2-targeted therapeutics.

RESULTS

Generation and Characterization of Heterologously Expressed Wild-Type and Mutant hCB2s

Stably transfected, polyclonal hCB2-HEK293 cell lines expressing either the wild-type (WT) or a cysteine-substitution receptor mutant were generated. Eight of the ten cysteine residues within the hCB2 TMHs and loop regions were modified either as single or double mutagenic lines to yield the hCB2 mutant series depicted in Figure 1B and listed in Table 1. Two EL2 cysteines, C174 and C179, were not mutated, for doing so abrogates ligand binding (Gouldson et al., 2000; Poso and Huffman, 2008; Zhang et al., 2005). Receptor binding competency was evaluated in saturation-binding assays carried out on membranes from each hCB2-HEK239 cell line with [^{3}H]-CP55940 radioligand, a well-recognized, universal reagent for cannabinoid receptor profiling in ligand-binding studies (Janero et al., 2009; Poso and Huffman, 2008). All recombinant WT and mutant hCB2s were capable of saturable [^{3}H]-CP55940 binding, with specific binding constituting 70%–90% of total binding, a proportion that allows reliable quantification of GPCR receptor affinity (K_d) and population density (B_{max}) (Bylund et al., 2004). The saturation-binding data (Table 1) indicate that hCB2s mutated in TMH2, IL2, EL2, TMH6, TMH7, or helix 8 (H8) by cysteine-to-serine (or -alanine) substitution have CP55940 binding affinities and membrane expression densities at least comparable to those of WT hCB2. The TMH1 mutant, C1.39(40)S, evidenced ~3-fold greater mean K_d (2.47 nM) and B_{max} (5.45 pmol/mg) values as compared to WT hCB2. Membranes from nontransfected HEK293 cells showed no specific CP55940 binding, demonstrating the lack of gross, nonspecific CP55940-membrane interaction (data not shown).

Binding Affinities of WT and Mutant hCB2s for AM1336

The affinities of WT and cysteine mutant hCB2s for AM1336 were determined in competitive binding assays using [^{3}H]-CP55940. As a covalent affinity probe (vide infra), AM1336 features an aliphatic side chain at the N^1 pyrazole nitrogen functionalized with a chemically reactive, electrophilic NCS group that invites, under our reaction conditions, its irreversible binding to hCB2 cysteine residues at (or immediately adjacent to) the ligand-binding pocket (Pei et al., 2008; Picone et al., 2005; Zvonok et al., 2008). Consequently, reported receptor affinities for AM1336 are considered "apparent K_i" (K_i*) values. Relative to WT hCB2, the hCB2 C175S, C7.38(284)A, C7.38(284)S, C7.42(288)A, C7.42(288)S, and C7.38(284)7.42(288)A mutants exhibited similar AM1336 binding affinities (Table 1). The hCB2 mutants C1.39(40)S, C2.59(89)S, C137S, and C313S evidenced moderate (~2-fold) decreases in affinity for AM1336, whereas the affinity of the C1.39(40)S mutant was reduced by ~3-fold.

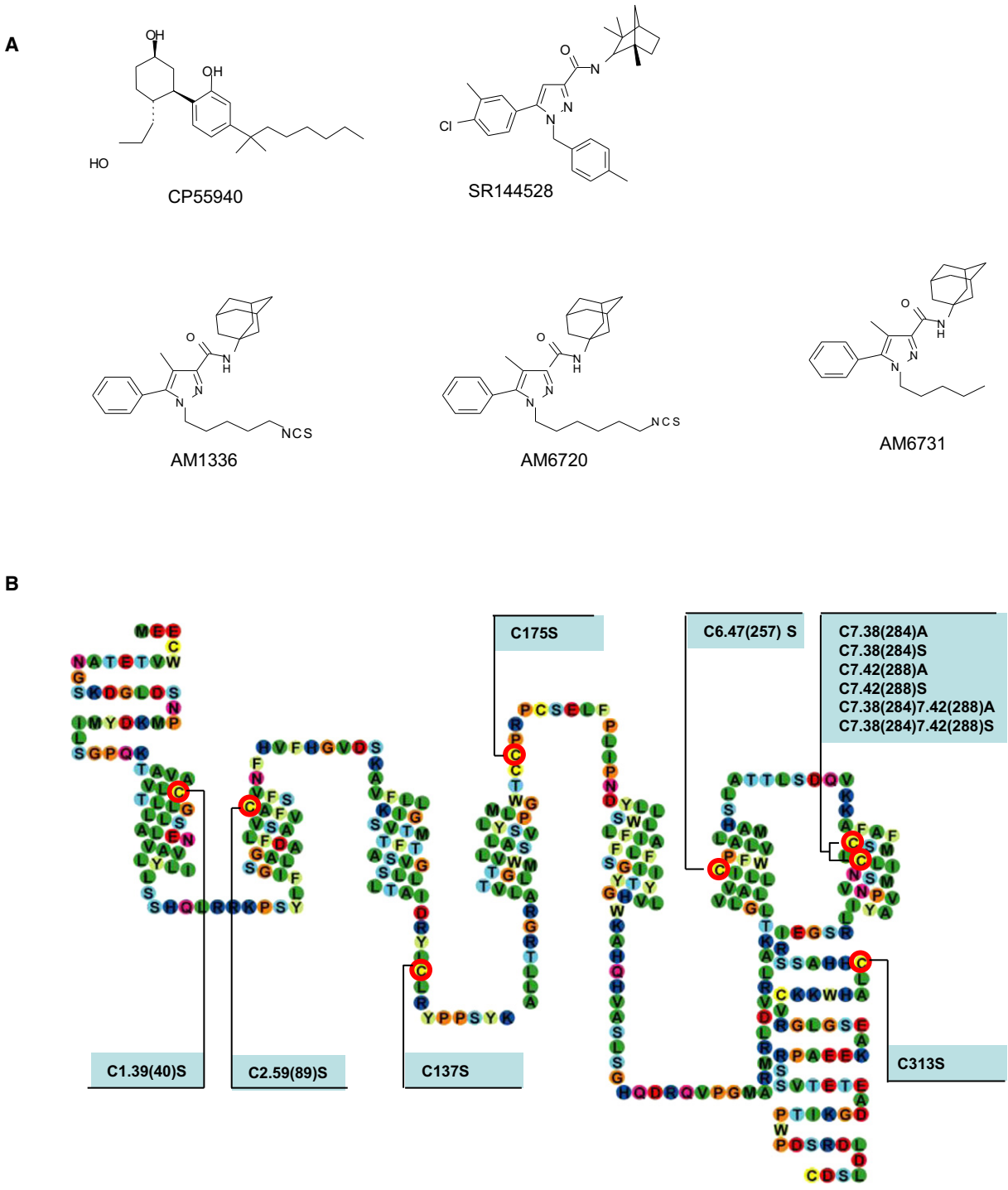

Figure 1. Structures of Cannabinoid Ligands and Serpentine Schematic Representation of hCB2

(A) Chemical structures of the principal cannabinoid ligands referred to in the text.

(B) Schematic representation of hCB2. The cysteine residues targeted for mutation in this study are denoted with a bold red circle, and the specific mutants generated are listed in the boxes above or below each respective locus.

Conversely, the binding affinities of C6.47(257)S and the double mutant C7.38(284)7.42(288)S for AM1336 were increased ~2-fold as compared to WT hCB2. The affinity of WT hCB2 for the nonfunctionalized AM1336 congener, AM6731 (K_i = 0.63 nM, 95% confidence interval [CI]: 0.44 ~0.81), was comparable to its apparent affinity (K_i*) for AM1336 (Table 1). Thus, the NCS group of AM1336 does not seem to interfere with its binding to hCB2.

Table 1. Ligand-Binding Parameters and AM1336 Binding Affinities of WT and Cysteine-Mutant hCB2s

	[^{3}H]-CP55940		AM1336
Receptor	K_d (nM)	B_{max} (pmol/mg)	K_i* (nM)
hCB2 WT	0.62	1.68	0.54
	(0.51–0.73)	(1.61–1.74)	(0.42–0.70)
hCB2 C1.39(40)S	2.47	5.45	2.21
	(1.86–3.01)	(4.99–5.92)	(1.75–2.79)
hCB2 C2.59(89)S	1.03	2.77	1.38
	(0.71–1.35)	(0.71–1.35)	(1.07–1.76)
hCB2 C137S	1.28	1.50	1.81
	(0.69–1.86)	(1.31–1.70)	(1.37–2.39)
hCB2 C175S	0.81	1.69	0.38
	(0.65–0.97)	(1.61–1.78)	(0.32–0.45)
hCB2 C6.47(257)S	0.96	1.58	0.12
	(0.78–1.14)	(1.50–1.66)	(0.10–0.14)
hCB2 C7.38(284)A	0.43	1.15	0.90
	(0.21–0.65)	(1.03–1.26)	(0.69–1.08)
hCB2 C7.38(284)S	0.76	1.28	0.40
	(0.58–0.94)	(1.21–1.36)	(0.25–0.65)
hCB2 C7.42(288)A	0.74	1.93	0.61
	(0.36–1.13)	(1.69–2.17)	(0.48–0.76)
hCB2 C7.42(288)S	1.01	1.07	0.35
	(0.79–1.22)	(1.01–1.13)	(0.28–0.45)
hCB2 C7.38(284)7.42(288)A	0.40	1.12	0.54
	(0.24–0.56)	(1.04–1.20)	(0.42–0.71)
hCB2 C7.38(284)7.42(288)S	1.45	1.38	0.19
	(1.09–1.80)	(1.28–1.48)	(0.14–0.25)
hCB2 C313S	1.18	1.07	1.33
	(0.89–1.48)	(1.01–1.13)	(1.04–1.70)

K_d and B_{max} values were derived from saturation-binding assays with [^{3}H]-CP55940 radioligand. Apparent binding affinities (K_i* values) for AM1336 were from competitive binding assays with [^{3}H]-CP55940. Both assays used membrane preparations from stably transfected HEK293 cells.. Data are the means of at least three independent experiments carried out in triplicate, with 95% confidence intervals shown in parentheses.

Covalent hCB2 Labeling

After 1 h preincubation of hCB2-HEK293 membranes with 5.4 nM AM1336 (i.e., 10-fold the hCB2 K_i* for AM1336; Table 1) at 30°C followed by extensive washing to remove unbound ligand, WT hCB2 displayed a significantly lower (by ~60%) mean B_{max} for [^{3}H]-CP55940 relative to parallel "control" membranes not exposed to AM1336 (Figure 2A). This result indicates that AM1336 demonstrated a 60% level of irreversible (covalent) binding to WT hCB2 such that [^{3}H]-CP55940 was subsequently unable to bind to those pre-occupied receptors. The hCB2 cysteine mutants C1.39(40)S, C2.59(89)S, C137S, C175S, C6.47(257)S, and C313S exhibited a comparable (53%–70%) extent of labeling by the AM1336 covalent affinity probe (Figure 2B). These comparative data allow conclusion that the specified cysteines in TMH1, TMH2, IL2, EL2, TMH6, and H8 are not critical determinants of AM1336 binding to hCB2. In contrast, the TMH7 single-cysteine mutants C7.38(284)A, C7.38(284)S, C7.42(288)A, and C7.42(288)S all showed significantly diminished labeling (28.5%, 33.5%, 39.0%, and 26.5%, respectively) by the covalent probe relative to control (Figures 2A and 2B). Mutation of both cysteines in TMH7 to alanine or serine [i.e., in the double mutants C7.38(284)C7.42(288)A or C7.38(284)C7.42(288)S] abrogated the covalent binding interaction between AM1336 and the receptor (Figures 2A and 2B). Additionally, preincubation of WT hCB2 with the nonfunctionalized (i.e., nonelectrophilic) AM1336 congener (AM6731) that is unable to bind covalently to hCB2 did not affect the receptor's B_{max} for [^{3}H]-CP55940 in a subsequent saturation-binding assay relative to control (data not shown), indicating that AM1336 does not irreversibly bind to hCB2 in the absence of its NCS group. In summary, these results provide strong, complimentary evidence that both TMH7 cysteines, C7.38(284) and C7.42(288), are sites of covalent attachment of the NCS moiety of AM1336 to hCB2 and, hence, are defining elements in the hCB2 binding landscape of the ligand.

Additional support for the importance of TMH7 cysteine residues to the hCB2 ligand-binding domain was obtained by profiling the interaction of WT hCB2 and hCB2 TMH7 cysteine mutants with AM6720, an AM1336 analog that carries a longer (by one carbon), NCS-terminal alkyl side chain (Figure 1A). The binding affinities of WT hCB2 and the hCB2 TMH7 cysteine mutants [C7.38(284)A, C7.38(284)S, C7.42(288)A, C7.42(288)S, C7.38(284)7.42(288)A, and C7.38(284)7.42(288)S] for AM6720 were similar (Table 2). Both AM1336 and AM6720 covalently labeled WT hCB2 to the same, comparably high extent (60% and 62%, respectively) (Figures 2B and 2C). However, the NCS moiety in AM6720 reacted with only one [i.e., C7.42(288)], but not the other [i.e., C7.38(284)], of the two hCB2 TMH7 cysteines with which AM1336 had reacted (Figure 2C).

Functional Characterization of WT and Mutant hCB2s

hCB2 is negatively coupled via $G_{i/o}$ to adenylyl cyclase, and CB2 inverse agonists (including SR144528) stimulate cellular forskolin-activated adenylyl cyclase activity (Rinaldi-Carmona et al., 1998). Thus, cellular cAMP production can be used as a functional assay for hCB2 activity (Bayewitch et al., 1995). AM6731, AM1336, and AM6720 increased forskolin-stimulated cAMP production concentration-dependently in cells expressing WT hCB2 receptor (Figure 3A), indicating that these three biarylpyrazole cannabinergic ligands act as hCB2 inverse agonists. Within a 95% CI, no difference was observed in the inverse-agonist potency (EC_{50}) of AM1336 among WT hCB2 and the single- and multiple-site hCB2 cysteine mutants (Table 3). However, the mean AM1336 maximum efficacy (E_{max}) for the C137S mutant and the two double-cysteine TMH7 mutants was ~2–3-fold less than the AM1336 E_{max} for WT hCB2 (Table 3 and Figure 3B). With respect to WT hCB2, the EC_{50} (19.54 nM) and E_{max} (368.5%) values of the non-functionalized inverse agonist, AM6731, were virtually identical to those of AM1336 (EC_{50} = 20.08 nM; E_{max} = 336.2% [Table 3]). In contrast, the AM1336 analog with the elongated, NCS-terminal aliphatic side chain (AM6720) evidenced a greater (by ~9-fold) mean EC_{50} (182.0 nM, 95% CI 131.6–244.0) and a comparable E_{max} (404.1%, 95% CI: 378.0–424.2) in comparison to AM1336.

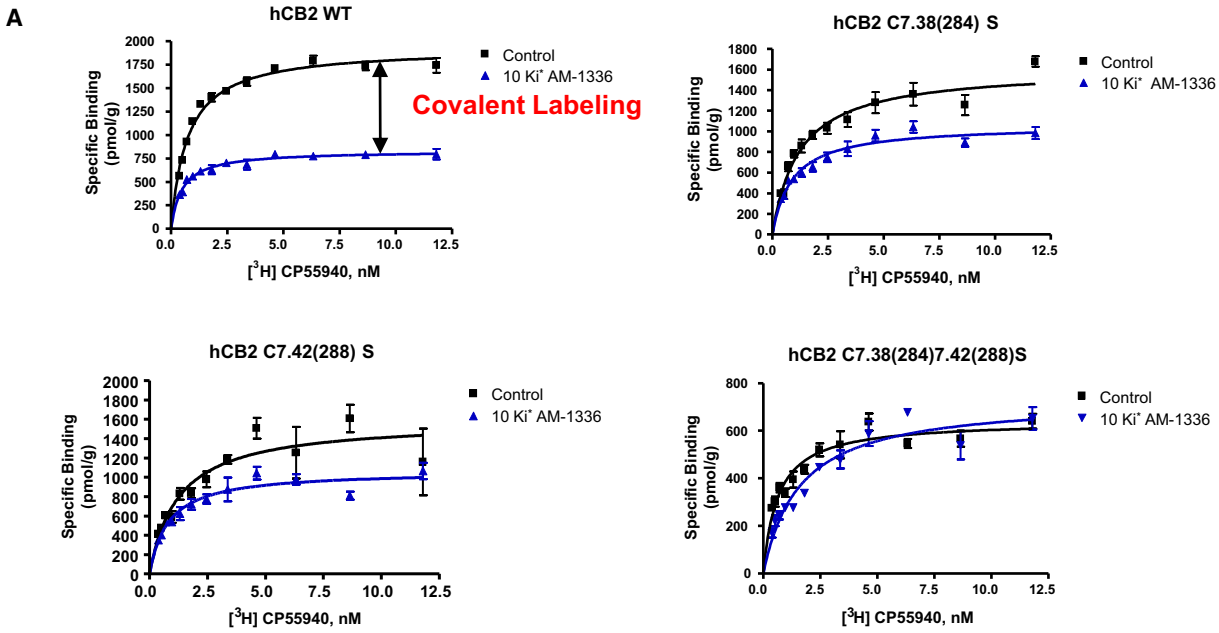
A
hCB2 WT
Specific Binding (pmol/g)
[3H] CP55940, nM
Control
10 Ki* AM-1336
Covalent Labeling
hCB2 C7.38(284) S
hCB2 C7.42(288) S
hCB2 C7.38(284)7.42(288)S

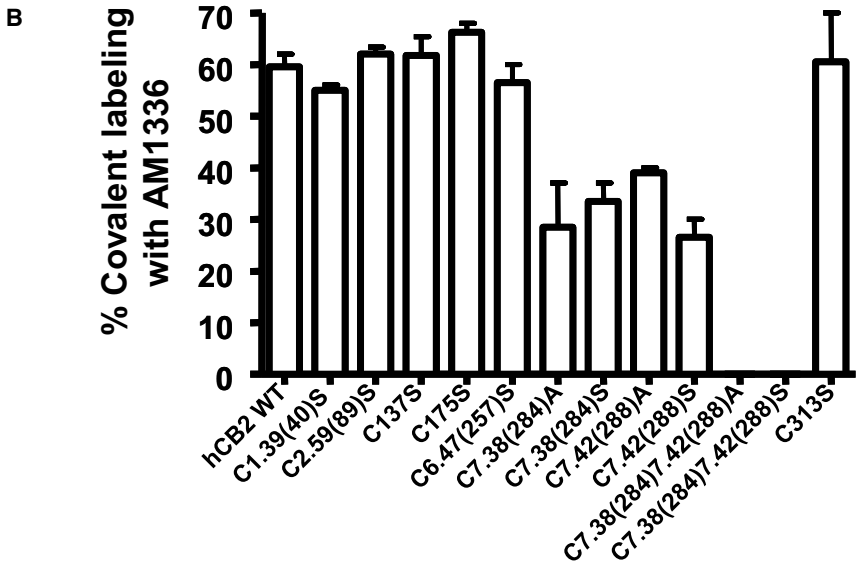
B
% Covalent labeling with AM1336
hCB2 WT
C1.39(40)S
C2.59(89)S
C137S
C175S
C6.47(257)S
C7.38(284)A
C7.38(284)S
C7.42(288)A
C7.42(288)S
C7.38(284)7.42(288)A
C7.38(284)7.42(288)S
C313S

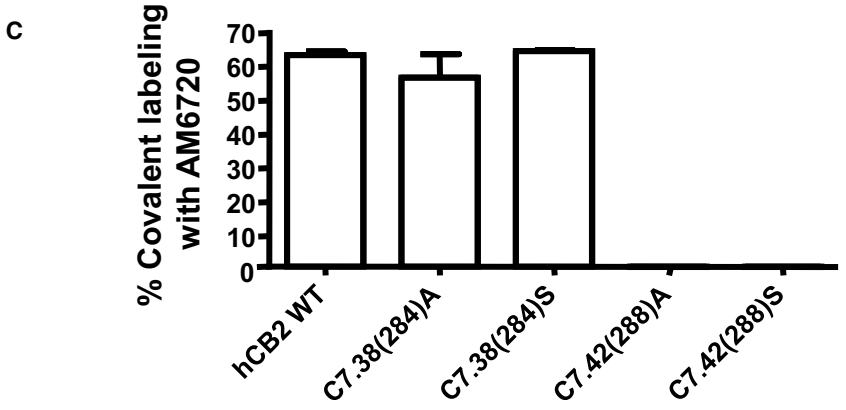
C
% Covalent labeling with AM6720
hCB2 WT
C7.38(284)A
C7.38(284)S
C7.42(288)A
C7.42(288)S

Table 2. Binding Affinities of WT and TMH7 Cysteine-Mutant hCB2s for AM1336 and AM6720 Using [^{3}H]-CP55940 as the Radioligand

	[^{3}H]-CP55940 K_i (nM)	
Receptor	AM1336	AM6720
hCB2 WT	0.54	1.03
	(0.42–0.70)	(0.85–1.25)
hCB2 C7.38(284)A	0.90	0.92
	(0.67–1.21)	(0.76–1.11)
hCB2 C7.38(284)S	0.40	0.87
	(0.25–0.65)	(0.72–1.05)
hCB2 C7.42(288)A	0.61	0.88
	(0.48–0.76)	(0.72–1.07)
hCB2 C7.42(288)S	0.35	0.73
	(0.28–0.45)	(0.54–0.98)

Binding affinities were determined in competitive binding assays using membrane preparations from stably transfected HEK293 cells. K_i values are the means of at least three independent experiments carried out in triplicate, with 95% confidence intervals shown in parentheses.

DISCUSSION

Although structure-function correlates of CB1, CB2, and peptides representing discrete holoreceptor domains have been investigated in reconstitution and homology-modeling studies, the crystal structures of these cannabinoid GPCRs have been elusive (Mukherjee et al., 2004; Pei et al., 2008; Tiburu et al., 2009a, 2009b; Zhang et al., 2005). Consequently, hCB2 structural features critical to ligand recognition and binding remain experimentally ill-defined, the translational importance of hCB2 as a drug target notwithstanding (Lunn et al., 2008; Poso and Huffman, 2008). To address this issue directly, we have used the LAPS experimental approach that we previously devised and successfully applied to interrogate enzyme and GPCR structure (Pei et al., 2008; Picone et al., 2005; Zvonok et al., 2008) along with a novel covalent affinity probe, the hCB2 biarylpyrazole antagonist/inverse agonist AM1336. An analog of the CB2 antagonists/inverse agonists SR144528 and AM6731, AM1336 was rationally designed and functionalized with an NCS moiety to react with specific amino acid residues at (or in the immediate microenvironment of) its hCB2 binding pocket. AM1336 thus represents the first covalent hCB2 antagonist/inverse agonist reported. Because neither the high affinity of AM1336 for hCB2 nor its EC_{50} and E_{max} as an hCB2 inverse agonist differ from those of its direct analog lacking the NCS moiety (i.e., AM6731), AM1336's chemically-reactive NCS group does not interfere with its binding to or functional interaction with hCB2.

As demonstrated previously for the LAPS paradigm with other NCS-functionalized cannabinoid probes (Pei et al., 2008; Picone et al., 2005; Zvonok et al., 2008), although lysine is in principle capable of interacting with an NCS group, the lysine amino group represents a significantly weaker nucleophile than the highly nucleophilic cysteine thiol under our reaction conditions (Picone et al., 2005). The potential for significant interaction between

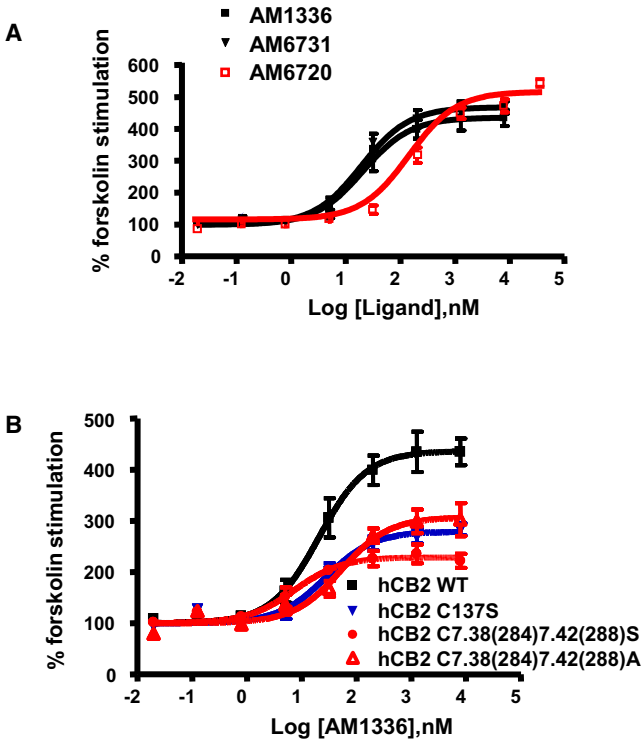

Figure 3. Concentration-Dependent Increase of Forskolin-Stimulated cAMP Accumulation in HEK293 Cells Expressing WT or Mutant hCB2s by Various Inverse Agonists

(A) Comparison among AM1336, AM6731, and AM6720 as inverse agonists of forskolin (5.0 μM)-stimulated cAMP accumulation in WT hCB2-HEK293 cells. (B) Comparison of the ability of AM1336 to increase forskolin (5.0 μM)-stimulated cAMP accumulation in HEK293 cells expressing either WT hCB2 or the hCB2 C137S, C7.38(284)7.42(288)S, or C7.38(284)7.42(288)A hCB2 mutant receptor. All data shown represent the means ± standard error of means of at least three independent experiments carried out in duplicate.

Figure 2. Labeling of WT and Mutant hCB2s with the Functionalized Covalent Affinity Probe AM1336 or AM6720

(A and B) Preincubation with AM1336 limits subsequent [^{3}H]-CP55940 binding to WT hCB2 (i.e., reduces the B_{max}) by ~60%. Select mutant hCB2s evidence either a reduction in the level of covalent labeling by AM1336 from this maximum [C7.38(284)A, C7.38(284)S, C7.42(288)A, C7.42(288)S], allowing greater subsequent binding of [^{3}H]-CP55940, or no AM1336 covalent labeling [C7.38(284)7.42(288)A and C7.38(284)7.42(288)S], allowing maximal subsequent [^{3}H]-CP55940 binding. Membranes prepared from HEK293 cells expressing either the WT or a designated mutant hCB2 were preincubated with 5.4 nM AM1336 (i.e., 10-fold its K_i* value) for 1 h at 30°C and washed extensively to remove noncovalently associated AM1336. The washed membranes were then subjected to a saturation binding assay using [^{3}H]-CP55940 as the radioligand. (A) Saturation-binding curves using [^{3}H]-CP55940 for WT and select mutant hCB2 receptors preincubated with AM1336 as described above (blue line) and control membranes processed in parallel, but without prior AM1336 exposure (black line). (B) Comparison of the difference in the [^{3}H]-CP55940 B_{max} values of each hCB2 receptor, designated as percent receptor covalent labeling by AM1336 with or without preincubation with AM1336.

(C) Covalent labeling of WT and select hCB2 mutant receptors with AM6720 at C7.42(288), but not C7.38(284), assessed with the protocol described above. All data shown represent the means with 95% confidence intervals of at least three independent experiments carried out in duplicate.

Table 3. Increase of Forskolin-Stimulated cAMP Accumulation in Cells Expressing WT or a Cysteine-Mutant hCB2

	AM1336	
	EC_{50} (nM)	E_{max} (%)
hCB2 WT	20.08	336.2
	(12.21–35.50)	(305.7–366.8)
hCB2 C1.39(40)S	59.31	375.9
	(28.27–124.4)	(324.3–427.5)
hCB2 C2.59(89)S	42.95	455.5
	(30.38–60.70)	(427.1–484.0)
hCB2 C137S	27.79	179.3
	(16.94–45.58)	(163.8–194.7)
hCB2 C175S	27.93	301.6
	(21.58–36.18)	(288.0–315.1)
hCB2 C6.47(257)S	36.27	435.4
	(18.71–70.32)	(384.0–486.7)
hCB2 C7.38(284)S	38.28	270.4
	(22.44–65.27)	(244.0–296.7)
hCB2 C7.42(288)S	30.63	233.8
	(13.64–68.74)	(200.6–267.0)
hCB2 C7.38(284)7.42(288)A	27.38	179.5
	(16.75–44.75)	(162.3–196.8)
hCB2 C7.38(284)7.42(288)S	7.49	129.0
	(3.62–15.50)	(114.4–143.6)
hCB2 C313S	19.44	513.8
	(10.62–35.59)	(461.3–566.4)

cAMP assays were carried out using cells from stably transfected hCB2-HEK293 WT and mutant lines. Data are mean EC_{50} and E_{max} values from at least three independent experiments carried out in triplicate with 95% confidence intervals shown in parentheses.

AM1336 and hCB2 lysines is rendered intrinsically remote by the fact that the only lysines modeled within the putative hCB2 binding pocket are in TMH3, a region unlikely on topological grounds to associate with the aliphatic side chain of a cannabinoid ligand (Chen et al., 2006; Gouldson et al., 2000). Indeed, we have recently demonstrated that the conserved hCB2 TMH3 lysine, K3.28(109), does not interact with the alkyl chain of AM841, a potent CB agonist and CP55940 analog (Pei et al., 2008).

Along with a high-affinity covalent probe, proteins that carry defined point mutations are other components of our LAPS experimental paradigm. In the current work, global cysteine to serine (and/or alanine) substitutions across hCB2 TMHs and two loop regions (IL2, EL2) allowed direct experimental assessment of the contribution of each cysteine to the hCB2 binding motif, as probed with AM1336. The hCB2 TMHs and loop regions contain a total of ten cysteines (Figure 1B). We elected not to mutate C174 and C179 in EL2 that apparently form a critical disulfide bridge essential to hCB2 ligand binding (Gouldson et al., 2000; Poso and Huffman, 2008; Zhang et al., 2005). The remaining eight were mutated to serine, both individually and, for the two TMH7 cysteines, in tandem. Introduction of serine into TMH7 by mutagenesis at C7.38(284) and/or C7.42(288) could invite interhelical hydrogen-bond formation between their side chains and nearby peptide-backbone carbonyl oxygens, leading to receptor deformation and artifactual alteration of its ligand-accommodation characteristics (Deupi et al., 2004). To obviate this potential problem, we also mutated these TMH7 cysteines to alanines. The comparable nature of the CP55940 and AM1336 binding profiles between the hCB2 TMH7 serine and alanine substitution mutants makes it unlikely that spurious, short-distance amino acid interactions were introduced as a result of the TMH7 cysteine-to-serine substitutions made. Because cysteine and serine are very conservative, isosteric analogs of each another and are characterized by polar, uncharged side chains, whereas alanine has a smaller, nonpolar aliphatic (i.e., methyl) side chain, this result further suggests that amino acid polarity and/or ligand side-chain bulk at TMH7 positions C7.38(284) and C7.42(288) do not appreciably influence hCB2-ligand interaction.

All hCB2 cysteine-substitution mutants generated demonstrated high binding affinities, favorable expression densities, and substantial (>70% total binding) specific binding in a standard saturation-binding assay using isolated cell membranes and [^{3}H]-CP55940 radioligand. Thus, the cysteine substitutions did not appear to compromise overall hCB2 structure, with the possible exception of the hCB2 C1.39(40)S mutant, which evidenced a somewhat lower CP55940 K_d as compared to WT hCB2. The comparable CP55940 binding affinities of the C7.38(284) and C7.42(288) single and double mutants suggest that these two TMH cysteine residues do not act synergistically. Furthermore, all hCB2 mutant receptors generated were functionally responsive to exogenously-introduced CB2 ligands in intact HEK293 cells, as evidenced by their effective signal transmission in a cell-based cAMP assay. Although we did not demonstrate directly (with, e.g., fluorescent probes [Dunham and Hall, 2009]) surface hCB2 expression in our HEK293 cell system, these data suggest that the proper trafficking dynamics and plasma-membrane disposition within HEK293 cells had occurred for the WT and hCB2 cysteine mutants studied. In contrast, Zhang et al. (2005) observed that hCB2 C1.39(40)S [and C4.67(175)A] mutants did not target the cell membrane in their HEK293-based expression system, a difference that could reflect, for example, a deficit of receptor-trafficking chaperones and/or accessory interacting proteins under their experimental conditions (Dunham and Hall, 2009; Niehaus et al., 2007) as well as compromised expression levels in their transfected constructs over time (Björk et al., 2005).

Virtually all of the hCB2 cysteine-substitution mutants exhibited an AM1336 K_i* comparable to that of WT hCB2. Therefore, the AM1336 binding site remained largely unaffected by these amino acid replacements, and no synergistic effect between the two TMH7 cysteine residues was apparent with respect to the hCB2-AM1336 molecular interaction. The largest difference in AM1336 binding affinity was evident between WT hCB2 and the C1.39(40)S mutant (K_i* values of 0.54 nM and 2.21 nM, respectively). This difference in AM1336 affinity, along with the difference in K_d of similar magnitude between WT hCB2 and the C1.39(40)S mutant for the nonclassical cannabinoid, CP55940, suggest that the C1.39 residue plays a permissive role in hCB2 binding of nonclassical and aminoalkylindole cannabinoid ligands. This result further illustrates the ability of CB2 to engage small molecules from several different chemical

classes at interaction sites considered distinct, yet with ligand-binding domains that may converge to varying extents and be influenced by similar, but not necessarily identical, factors at the molecular level (Janero et al., 2009; Lunn et al., 2008; Palmer et al., 2002; Pei et al., 2008; Poso and Huffman, 2008).

This study used the nonfunctionalized direct AM1336 congener, AM6731, as the control ligand, an approach consonant with the use of small-molecule probes in chemical biology to explore protein structure/function (Frye, 2010). Prior work (Pei et al., 2008) demonstrates that: (1) the affinities of WT hCB2 and the hCB2 C6.47(257)S mutant for the tricyclic classical cannabinoid agonist Δ^9-THC are comparable in competitive binding assays with either [^{3}H]-CP-55940 or [^{3}H]-WIN55212-2; and (2) the hCB2 C6.47(257)S mutant, relative to WT hCB2, displays a significantly increased (by 2-3-fold) affinity for the biarylpyrazole inverse agonist SR144528 in a competitive binding assay with [^{3}H]-WIN55212-2. These results help place the recent findings with AM1336 into a broader ligand context. Specifically, the hCB2 C6.47(257)S mutant shows an increased affinity for both inverse agonists SR144528 (Pei et al., 2008) and AM1336 (Table 1), whereas mutation of this TMH6 cysteine residue did not alter the receptor's affinity for Δ^9-THC agonist (Pei et al., 2008). These comparative data suggest that some features of the hCB2 binding site may be shared between AM1336 and other hCB2 biarylpyrazole inverse agonists, but not with classical tricyclic agonists. The suggestion notwithstanding, overlapping cannabinoid GPCR binding sites for ligands of different chemical structures need not be identical (Gouldson et al., 2000). This concept is noteworthy here, for the chemical structure of AM1336 is changed significantly from that of SR144528 through replacement of the latter's aromatic (4-methylphenyl) methyl substituent at the N^1 pyrazole nitrogen with an NCS-functionalized alkyl chain. Future experimental definition of the optimal binding poses and their determinants for a wide variety of hCB2 agonists/antagonists with divergent chemical structures would assist the rational design of hCB2 ligands as pharmacologically attractive drugs with, perhaps, functional selectivity downstream from hCB2. Our LAPS approach, supplemented by modeling studies with AM1336, AM6731, and other (covalent) ligands along with progressive refinement of extant CB2 homology models (Durdagi et al., 2009; Pei et al., 2008), offers a tenable route to such data.

We previously demonstrated the importance of hCB2 C6.47 (257) to the remarkable potency of an NCS-derivatized classical cannabinoid agonist, AM841, a phenomenon that directly reflects covalent AM841 binding to that TMH6 residue (Pei et al., 2008). The present study offers experimental demonstration that two TMH7 cysteine residues [i.e., C7.38(284) and C7.42(288)] can establish a productive binding interaction between hCB2 and the NCS-functionalized covalent affinity probe and inverse agonist, AM1336, without enhancing its inverse-agonist activity relative to the nonderivatized parent, AM6731. An AM1336 analog with a longer, NCS-functionalized alkyl tail (AM6720) interacts only with C7.38(284), which is positioned further down in the TMH7 bundle. Although the role of hCB2 C6.47(257) in AM841 binding is similar to that of hCB1 C6.47(355) (Pei et al., 2008), the involvements of hCB2 C7.38(284) in AM1336 binding and hCB2 C7.42(288) in AM1336 and AM6720 binding have no apparent direct correlates in hCB1. These results further support our previous contention (Pei et al., 2008) that both the binding domains of hCB2 ligands with distinct pharmacological modes of action as well as differences in ligand-binding motifs between hCB1 and hCB2 can be distinguished at the amino acid level with our LAPS experimental approach. This view is further substantiated by our finding that hCB1 does not bind AM1336 irreversibly (data not shown), suggesting that the hCB1 and hCB2 ligand-binding domains differ with respect to critical cysteine residues.

Results from a cell-based cAMP assay substantiate that WT and mutant hCB2s retain functionality when overexpressed in our HEK293 cell system. Although it is not the aim of the current work to detail the pharmacology and cellular signaling route(s) of the WT or cysteine mutant hCB2s in HEK293 cells, the cAMP data offer provisional functional evidence that the high-affinity AM1336 probe displays an inverse-agonist action against the WT and hCB2 cysteine point mutants studied. In a saturation-binding assay with CP55940, expression densities were at least comparable among the WT and all mutant hCB2s, notably including the two mutant receptors identified by LAPS as having point-mutations in cysteines critical to probe (AM1336) interaction [i.e., C7.38(284)and C7.42(288)] (Table 1). Both the naive parental HEK cells and the HEK cells transfected with and overexpressing either WT and any hCB2 mutant contain very low amounts of cAMP (data not shown); neither forskolin nor AM1336 affects the low cAMP content of naive parental HEK cells not overexpressing WT or mutant hCB2 (data not shown); and the hCB2-HEK293 cAMP experiments described herein were conducted in the absence of exogenous hCB2 agonist. These characteristics of our cell-based hCB2 expression system render the forskolin cAMP response we observe indicative of the constitutive activity of WT and mutant hCB2s (Jansson et al., 1998; Kozell and Neve, 1997; Shryock et al., 1998). Indeed, it is likely that the amplifying action of forskolin on adenylyl cyclase allied to hCB2 overexpression enabled us to detect the constitutive receptor activity (Kollias-Baker et al., 1997). In HEK cells overexpressing either WT or any mutant hCB2, 5.0 μM forskolin strongly stimulates cellular cAMP production, bringing the cellular cAMP content in each hCB2-HEK293 cell construct to a comparably high level before AM1336 exposure, and AM1336 effectively stimulates the forskolin-potentiated cAMP formation in HEK cells overexpressing either WT or any mutant hCB2 with equivalently high (nanomolar) potency (IC_{50} data in Table 3). If there were differences in constitutive activity between the WT and mutant hCB2s as overexpressed in the HEK cells, the 5.0 μM forskolin treatment would have resulted in markedly disparate levels of cAMP at stimulated baseline among cells expressing the WT or a mutant hCB2, which was not the case. Furthermore, the AM1336 functional sensitivity would be highly variable among WT and mutant receptors, counter to the observed, comparable EC_{50}'s of this high-affinity CB2 ligand against both the WT and all mutant hCB2s in the cellular cAMP assay (Table 3). Based on this reasoning as supported by literature precedent in other cell-based cAMP assay systems overexpressing WT and mutant/subtype GPCRs (Ben-Shlomo et al., 2009; Benned-Jensen and Rosenkilde, 2008; Portier et al., 1999; Shen et al., 2006; Wieland et al., 2001), we conclude from the aggregate cAMP data that the constitutive functional activity of WT hCB2 is conserved and displayed to a similar

degree in the WT and cysteine-mutant hCB2s we have studied such that the potentiation of forskolin-stimulated cAMP in HEK293 cells overexpressing each receptor by AM1336 is suggestive of an inverse-agonist property of this high-affinity hCB2 chemical probe.

The hCB2 cysteine-to-serine substitutions did not significantly change AM1336's inverse-agonist potency (indexed as EC_{50}). The fact that the AM1336 NCS group reacts with either hCB2 C7.38(284) or C7.42(288) and maintains full pharmacological function of the ligand implies that this region of the hCB2 binding pocket exhibits a degree of structural plasticity. The ligand accommodation capability of this region, however, may be circumscribed, for the maximal AM1336 inverse-agonist efficacy (indexed as E_{max}) was moderately decreased in the double C7.38(284)7.42(288)A and C7.38(284)7.42(288)S mutants. It is unlikely that the lower AM1336 E_{max} of the C7.38(284)C7.42(288)A and C7.38(284)C7.42(288)S double mutants reflects a compromised covalent interaction between these receptors and AM1336, for the non-functionalized analog of AM1336 that does not covalently bind to hCB2 (AM6731) exhibited an E_{max} (and EC_{50}) comparable to that of AM1336. Rather, the fact that WT hCB2 evidenced a much higher (9-fold) EC_{50} and similar E_{max} for the AM1336 analog with a longer side chain (AM6720) as compared to AM1336 itself suggests that a functionally optimal binding interaction of this family of antagonist/inverse agonist ligands with hCB2 involves a binding domain that most readily accommodates an aliphatic side chain of five carbons in length and involves a TMH7 binding interaction with either C7.38(284) or C7.42(288). Maximal AM1336 inverse-agonist efficacy (E_{max}) was also decreased in the single hCB2 C3.56(137)S mutant. The C3.56(137) residue, which is located downstream from the highly-conserved DRY (Asp-Arg-Tyr) motif at the cytoplasmic terminus of TMH3, has been generally implicated in the interactions between GPCRs and G protein subunits that support information relay from the extra-to the intracellular compartment (Feng and Song, 2003). Therefore, mutating C3.56(137) may have limited the receptor's functionality such that antagonist interaction with it would elicit at most a dampened maximal effect.

SIGNIFICANCE

The hCB2 receptor is emerging as one of the most interesting GPCR drug targets in translational biomedicine. Antagonists of hCB2-mediated signal transmission hold therapeutic potential as immunomodulatory and anti-inflammatory drugs. Yet hCB2 remains intractable for high-resolution structure determination. Thorough understanding of the molecular interactions between hCB2 and small-molecule, high-affinity orthosteric modulators would greatly facilitate the rational design and therapeutic exploitation of hCB2-targeted antagonists. Despite extant data from pharmacological structure-activity studies and homology modeling, direct experimental hCB2 structural information is lacking. The present work has used our LAPS experimental paradigm integrating a chemically selective affinity probe as the first covalent hCB2 antagonist/inverse agonist (AM1336) and site-directed mutational analysis. These complimentary approaches have enabled us to define the role of cysteine residues in the interaction of this biarylpyrazole ligand with functionally-active hCB2. Our data directly demonstrate the influence of C1.39(40) and C137 and the importance of C7.38(284) and 7.42(288)S residues in hCB2 ligand recognition and optimal pharmacological antagonism/inverse agonism by AM1336. We have also identified specific hCB2 features at the amino acid level affecting hCB2-ligand interaction and function not shared by CB1. These results help inform the rational design of targeted, selective hCB2 small-molecule modulators with therapeutic potential. The data supplement the very limited experimentally-derived structural detail for GPCRs, cell-surface molecules constituting the largest family of proteins in the human genome and one of the most frequently addressed classes of drug targets.

EXPERIMENTAL PROCEDURES

Materials

Sources are given in the Supplemental Experimental Procedures available online.

Amino Acid Numerical Descriptor

Amino acid residues in hCB2 TMHs are numbered using a modified Ballesteros and Weinstein (1995) system. The most highly conserved residue in each TMH is assigned a locant of 50. This number is preceded by the TMH number and followed in parentheses by the sequence number. All other residues in any given TMH are numbered relative to this residue.

Site-Directed Mutagenesis, Cell Transfection and Culture, and Transgene Integrity

The partial-length cDNA encoding the hCB2 translated region was kindly provided by Dr. Sean Munro (MRC Laboratory of Molecular Biology, Cambridge, UK). Techniques utilized to construct hCB2 mutants and express WT and mutant hCB2s in HEK293 cells were essentially those detailed (Pei et al., 2008), as described in the Supplemental Experimental Procedures.

Cell Membrane Preparation and Receptor Binding Assays

After cell disruption by cavitation in a pressure cell at 65 Torr, cell membranes were isolated by ultracentrifugation and stored at −70°C (Xu et al., 2005). Receptor ligand-binding assays were essentially as described (Lan et al., 1999; Pei et al., 2008) and detailed in the Supplemental Experimental Procedures.

Receptor Affinity Labeling

Covalent affinity labeling was carried out with hCB2-HEK293 membranes prepared as described above. Membrane (1 mg protein/ml) in TME-BSA was allowed to equilibrate with either an NCS-derivatized ligand (i.e., AM1336 or AM6720) or the underivatized, direct analog of AM1336 (i.e., AM6731) as negative control for 1 h at 30°C with agitation (total volume, ~2.5 ml). Final ligand concentration was 10-fold its respective K_i. The reaction mixture was centrifuged at 27,000 × g, 30°C, and the resulting membrane pellet was washed three times with 10 ml TME-BSA at 30°C to remove any unbound ligand. The membranes were allowed to equilibrate at 30°C in 25 ml TME-BSA for 15 min between each wash. Next, three final washes were conducted with the same protocol, but with BSA-free TME. Saturation-binding assays were then carried out with the washed membranes and [^{3}H]-CP55940 radioligand, and the B_{max} for each membrane sample was calculated, as described above. Percent covalent labeling was calculated as: $\{[B_{max(control)} - B_{max(labeled)}]/B_{max(control)}\} \times 100$. The $B_{max(control)}$ for [^{3}H]-CP55940 was determined by conducting the assay exactly as described, but in the absence of test ligand (i.e., AM1336, AM6720, or AM6731).

cAMP Assay

Receptor functionality was indexed as cAMP formation in a cell-based bioassay modified from Tao et al. (1999) and detailed in the Supplemental Experimental Procedures.

SUPPLEMENTAL INFORMATION

Supplemental Information includes Supplemental Experimental Procedures and can be found with this article online at doi:10.1016/j.chembiol.2010.08.010.

ACKNOWLEDGMENTS

This work has been supported by the National Institutes of Health, National Institute on Drug Abuse (DA9158 and DA3801 to A.M.).

Received: February 8, 2010
Revised: August 9, 2010
Accepted: August 12, 2010
Published: October 28, 2010

REFERENCES

Anand, P., Whiteside, G., Fowler, C.J., and Hohmann, A.G. (2009). Targeting CB_2 receptors and the endocannabinoid system for treatment of pain. Brain. Res. Rev. *60*, 255–266.

Ballesteros, J.A., and Weinstein, H. (1995). Integrated methods for the construction of three dimensional models and computational probing of structure function relations in G protein-coupled receptors. In Methods in Neuroscience, *Volume 25*, P.M. Conn and S.M. Sealfon, eds. (San Diego, CA: Academic Press), pp. 366–428.

Bayewitch, M., Avidor-Reiss, T., Levy, R., Barg, J., Mechoulam, R., and Vogel, Z. (1995). The peripheral cannabinoid receptor: adenylate cyclase inhibition and G protein coupling. FEBS Lett. *375*, 143–147.

Ben-Shlomo, A., Zhou, C., Pichurin, O., Chesnokova, V., Liu, N.-A., Culler, M.D., and Melmed, S. (2009). Constitutive somatostatin receptor activity determines tonic pituitary cell response. Mol. Endocrinol. *23*, 337–348.

Benned-Jensen, T., and Rosenkilde, M.M. (2008). Structural motifs of importance for the constitutive activity of the orphan 7TM receptor EBI2: analysis of receptor activation in the absence of an agonist. Mol. Pharmacol. *74*, 1008–1021.

Björk, S., Vainio, M., and Scheinin, M. (2005). Uneven cellular expression of recombinant alpha2A-adrenoceptors in transfected CHO cells results in loss of response in adenylyl cyclase inhibition. Biochim. Biophys. Acta *1744*, 38–46.

Bylund, D.B., Deupree, J.D., and Toews, M.L. (2004). Radioligand-binding methods for membrane preparations and intact cells. Methods Mol. Biol. *259*, 1–28.

Chen, J.Z., Han, X.W., Liu, Q., Makriyannis, A., Wang, J., and Xie, X.Q. (2006). 3D-QSAR studies of arylpyrazole antagonists of cannabinoid receptor subtypes CB1 and CB2. A combined NMR and CoMFA approach. J. Med. Chem. *49*, 625–636.

Congreve, M., and Marshall, F. (2010). The impact of GPCR structures on pharmacology and structure-based drug design. Br. J. Pharmacol. *159*, 986–996.

Dainese, E., Oddi, S., and Maccarrone, M. (2008). Lipid-mediated dimerization of β_2-adrenergic receptor reveals important clues for cannabinoid receptors. Cell. Mol. Life Sci. *65*, 2277–2279.

Dalton, G.D., Bass, C.E., Van Horn, C.G., and Howlett, A.C. (2009). Signal transduction via cannabinoid receptors. CNS Neurol. Disord. Drug Targets *8*, 422–431.

Deupi, X., Olivella, M., Govaerts, C., Ballesteros, J.A., Campillo, M., and Pardo, L. (2004). Ser and Thr residues modulate the conformation of pro-kinked transmembrane α-helices. Biophys. J. *86*, 105–115.

Di Marzo, V. (2009). The endocannabinoid system: its general strategy of action, tools for its pharmacological manipulation and potential therapeutic exploitation. Pharmacol. Res. *60*, 77–84.

Dunham, J.H., and Hall, R.A. (2009). Enhancement of the surface expression of G protein-coupled receptors. Trends Biotechnol. *27*, 541–545.

Durdagi, S., Papadopoulos, M.G., Zoumpoulakis, P.G., Koukoulitsa, C., and Mavromoustakos, T. (2009). A computational study on cannabinoid receptors and potent bioactive cannabinoid ligands: homology modeling, docking, de novo drug design and molecular dynamics analysis. Mol. Divers. *14*, 257–276.

Feng, W., and Song, Z.H. (2003). Effects of D3.49A, R3.50A, and A6.34E mutations on ligand binding and activation of the cannabinoid-2 (CB2) receptor. Biochem. Pharmacol. *65*, 1077–1085.

Frye, S.V. (2010). The art of the chemical probe. Nat. Chem. Biol. *6*, 159–161.

Gouldson, P., Calandra, B., Legoux, P., Kerneis, A., Rinaldi-Carmona, M., Barth, F., Le Fur, G., Ferrara, P., and Shire, D. (2000). Mutational analysis and molecular modelling of the antagonist SR144528 binding site on the human cannabinoid CB(2) receptor. Eur. J. Pharmacol. *401*, 17–25.

Hanson, M.A., and Stevens, R.C. (2009). Discovery of new GPCR biology: one receptor structure at a time. Structure *17*, 8–14.

Janero, D.R., and Makriyannis, A. (2009). Cannabinoid receptor antagonists: pharmacological opportunities, clinical experience, and translational prognosis. Expert Opin. Emerg. Drugs *14*, 43–65.

Janero, D.R., Vadivel, S.K., and Makriyannis, A. (2009). Pharmacotherapeutic modulation of the endocannabinoid signaling system in psychiatric disorders: drug-discovery strategies. Int. Rev. Psychiatry *21*, 122–133.

Jansson, C.C., Kukkonen, J.P., Näsman, J., Huifang, G.E., Wurster, S., Virtanen, R., Savola, J.-M., Cockcroft, V., and Åkerman, K.E.O. (1998). Protean agonism at α_{2A}-adrenoreceptors. Mol. Pharmacol. *53*, 963–968.

Kokkola, T., Savinainen, J.R., Mönkkönen, K.S., Retamal, M.D., and Laitinen, J.T. (2005). S-nitrosothiols modulate G protein-coupled receptor signaling in a reversible and highly receptor-specific manner. BMC Cell Biol. *6*, 21.

Kollias-Baker, C.A., Ruble, J., Jacobson, M., Harrison, J.K., Ozeck, M., Shryock, J.C., and Belardinelli, L. (1997). Agonist-independent effect of an allosteric enhancer of the A_1 adenosine receptor in CHO cells stably expressing the recombinant human A_1 receptor. J. Pharmacol. Exp. Ther. *281*, 761–768.

Kozell, L.B., and Neve, K.A. (1997). Constitutive activity of a chimeric D_2/D_1 dopamine receptor. Mol. Pharmacol. *52*, 1137–1149.

Lan, R., Liu, Q., Fan, P., Lin, S., Fernando, S.R., McCallion, D., Pertwee, R., and Makriyannis, A. (1999). Structure-activity relationships of pyrazole derivatives as cannabinoid receptor antagonists. J. Med. Chem. *42*, 769–776.

Liu, Q.R., Pan, C.H., Hishimoto, A., Li, C.Y., Xi, Z.X., Llorente-Berzal, A., Viveros, M.P., Ishiguro, H., Arinami, T., Onaivi, E.S., and Uhl, G.R. (2009). Species differences in cannabinoid receptor 2 (CNR2 gene): identification of novel human and rodent CB2 isoforms, differential tissue expression and regulation by cannabinoid receptor ligands. Genes Brain Behav. *8*, 519–530.

Lunn, C.A., Reich, E.-P., Fine, J.S., Lavey, B., Kozlowski, J.A., Hipkin, R.W., Lundell, D.J., and Bober, L. (2008). Biology and therapeutic potential of cannabinoid CB_2 receptor inverse agonists. Br. J. Pharmacol. *153*, 226–239.

Miller, A.M., and Stella, N. (2008). CB_2 receptor-mediated migration of immune cells: it can go either way. Br. J. Pharmacol. *153*, 299–308.

Mukherjee, S., Adams, M., Whiteaker, K., Daza, A., Kage, K., Cassar, S., Meyer, M., and Yao, B.B. (2004). Species comparison and pharmacological characterization of rat and human CB2 cannabinoid receptors. Eur. J. Pharmacol. *505*, 1–9.

Niehaus, J.L., Liu, Y., Wallis, K.T., Egertová, M., Bhartur, S.G., Mukhopadhyay, S., Shi, S., He, H., Selley, D.E., Howlett, A.C., et al. (2007). CB_1 cannabinoid receptor activity is modulated by the cannabinoid receptor interacting protein CRIP 1a. Mol. Pharmacol. *72*, 1557–1566.

Palmer, S.L., Thakur, G.A., and Makriyannis, A. (2002). Cannabinergic ligands. Chem. Phys. Lipids *121*, 3–19.

Pei, Y., Mercier, R.W., Anday, J.K., Thakur, G.A., Zvonok, A.M., Hurst, D., Reggio, P.H., Janero, D.R., and Makriyannis, A. (2008). Ligand-binding architecture of human CB2 cannabinoid receptor: Evidence for receptor

subtype-specific binding motif and modeling GPCR activation. Chem. Biol. *15*, 1207–1219.

Picone, R.P., Khanolkar, A.D., Xu, W., Ayotte, L.A., Thakur, G.A., Hurst, D.P., Abood, M.E., Reggio, P.H., Fournier, D.J., and Makriyannis, A. (2005). (-)-7′-Isothiocyanato-11-hydroxy-1′,1′-dimethylheptylhexahydrocannabinol (AM841), a high-affinity electrophilic ligand, interacts covalently with a cysteine in helix six and activates the CB1 cannabinoid receptor. Mol. Pharmacol. *68*, 1623–1635.

Portier, M., Rinaldi-Carmona, M., Pecceu, F., Combres, T., Poinot-Chazel, C., Calandra, B., Barth, F., Le Fur, G., and Casellas, P. (1999). SR144528, an antagonist for the peripheral cannabinoid receptor that behaves as an inverse agonist. J. Pharmacol. Exp. Ther. *288*, 582–589.

Poso, A., and Huffman, J.W. (2008). Targeting the cannabinoid CB2 receptor: modeling and structural determinants of CB2 selective ligands. Br. J. Pharmacol. *153*, 335–346.

Rahn, E.J., Zvonok, A.M., Thakur, G.A., Khanolkar, A.D., Makriyannis, A., and Hohmann, A.G. (2008). Selective activation of cannabinoid CB_2 receptors suppresses neuropathic nociception induced by treatment with the chemotherapeutic agent paclitaxel in rats. J. Pharmacol. Exp. Ther. *327*, 584–591.

Rinaldi-Carmona, M., Barth, F., Millan, J., Derocq, J.-M., Casellas, P., Cogny, C., Oustric, D., Sarran, M., Bouaboula, M., Calandra, B., et al. (1998). SR 144528, the first potent and selective antagonist of the CB2 cannabinoid receptor. J. Pharmacol. Exp. Ther. *284*, 644–650.

Shen, C.-P., Xiao, J.C., Armstrong, H., Hagmann, W., and Fong, T.M. (2006). F200A substitution in the third transmembrane helix of human cannabinoid CB_1 receptor converts AM2233 from receptor agonist to inverse agonist. Eur. J. Pharmacol. *531*, 41–46.

Shire, D., Calandra, B., Bouaboula, M., Barth, F., Rinaldi-Carmona, M., Casellas, P., and Ferrara, P. (1999). Cannabinoid receptor interaction with the antagonists SR 141716A and SR 144528. Life Sci. *65*, 627–635.

Shryock, J.C., Ozeck, M.J., and Belardinelli, L. (1998). Inverse agonists and neutral antagonists of recombinant human A_1 adenosine receptors stably expressed in Chinese hamster ovary cells. Mol. Pharmacol. *53*, 886–893.

Tao, Q., McAllister, S.D., Andreassi, J., Nowell, K.W., Cabral, G.A., Hurst, D.P., Bachtel, K., Ekman, M.C., Reggio, P.H., and Abood, M.E. (1999). Role of a conserved lysine residue in the peripheral cannabinoid receptor (CB2): evidence for subtype specificity. Mol. Pharmacol. *55*, 605–613.

Tiburu, E.K., Gulla, S.V., Tiburu, M., Janero, D.R., Budil, D.E., and Makriyannis, A. (2009a). Dynamic conformational responses of a human cannabinoid receptor-1 helix domain to its membrane environment. Biochemistry *48*, 4895–4904.

Tiburu, E.K., Tyukhtenko, S., Deshmukh, L., Vinogradova, O., Janero, D.R., and Makriyannis, A. (2009b). Structural biology of human cannabinoid receptor-2 helix 6 in membrane-mimetic environments. Biochem. Biophys. Res. Commun. *384*, 243–248.

Topiol, S., and Sabio, M. (2009). X-ray structure breakthroughs in the GPCR transmembrane region. Biochem. Pharmacol. *78*, 11–20.

Wieland, K., Bongers, G., Yamamoto, Y., Hashimto, T., Yamatodani, A., Menge, W.M.B.P., Timmerman, H., Lovenberg, T.W., and Leurs, R. (2001). Constitutive activity of histamine H_3 receptors stably expressed in SK-N-MC cells: display of agonism and inverse agonism by H_3 antagonists. J. Pharmacol. Exp. Ther. *299*, 908–914.

Xu, W., Filppula, S.A., Mercier, R., Yaddanapudi, S., Pavlopoulos, S., Cai, J., Pierce, W.M., and Makriyannis, A. (2005). Purification and mass spectroscopic analysis of human CB1 cannabinoid receptor functionally expressed using the baculovirus system. J. Pept. Res. *66*, 138–150.

Zhang, R., Hurst, D.P., Barnett-Norris, J., Reggio, P.H., and Song, Z.H. (2005). Cysteine 2.59(89) in the second transmembrane domain of human CB2 receptor is accessible within the ligand binding crevice: evidence for possible CB2 deviation from a rhodopsin template. Mol. Pharmacol. *68*, 69–83.

Zvonok, N., Pandarinathan, L., Williams, J., Johnston, M., Karageorgos, I., Janero, D.R., Krishnan, S.C., and Makriyannis, A. (2008). Covalent inhibitors of human monoacylglycerol lipase: ligand-assisted characterization of the catalytic site by mass spectrometry and mutational analysis. Chem. Biol. *15*, 854–862.

Zvonok, N., Xu, W., Williams, J., Janero, D.R., Krishnan, S.C., and Makriyannis, A. (2010). Mass spectrometry-based GPCR proteomics: comprehensive characterization of the human cannabinoid 1 receptor. J. Proteome Res. *9*, 1746–1753.

